Local Magnetism and Spin Dynamics of the Frustrated Honeycomb Rhodate Li_2RhO_3

P. Khuntia,[1,*] S. Manni,[2,†] F. R. Foronda,[3] T. Lancaster,[4] S. J. Blundell,[3] P. Gegenwart,[2] and M. Baenitz[1,‡]

[1]*Max Planck Institute for Chemical Physics of Solids, 01187 Dresden, Germany*
[2]*EP VI, Center for Electronic Correlations and Magnetism, Augsburg University, D-86159 Augsburg, Germany*
[3]*Oxford University Department of Physics, Clarendon Laboratory, Parks Road, Oxford OX1 3PU, United Kingdom*
[4]*Durham University, Centre for Materials Physics, South Road, Durham, DH1 3LE, United Kingdom*

(Dated: April 9, 2018)

We report magnetization, heat capacity, ^{7}Li nuclear magnetic resonance (NMR) and muon-spin rotation (μSR) measurements on the honeycomb 4d^5 spin liquid candidate Li_2RhO_3. The magnetization in small magnetic fields provides evidence for a partial spin freezing of a small fraction of Rh^{4+} moments at 6 K whereas the Curie-Weiss behavior above 100 K suggests a pseudo-spin–1/2 paramagnet with a moment of about 2.2 μ_B. The magnetic specific heat (C_m) exhibits no field dependence and demonstrates the absence of long range magnetic order down to 0.35 K. C_m/T passes through a broad maximum at about 10 K and $C_m \propto T^2$ at low temperature. Measurements of the spin-lattice relaxation rate ($1/T_1$) reveal a gapless slowing down of spin fluctuations on cooling with $1/T_1 \sim T^{2.2}$. The results from NMR and μSR are consistent with a scenario in which a minority of Rh^{4+} moments are in a short-range correlated frozen state and coexist with a majority of moments in a liquid-like state that continue to fluctuate at low temperature.

PACS numbers: 75.10.Jm, 75.10.Kt, 76.60.-k, 76.60.Es, 76.75.+i
Keywords: NMR, μSR, Magnetization, Specific Heat, Quantum Spin Liquid, and Spin Orbit Interaction

arXiv:1512.04904v4 [cond-mat.str-el] 26 Sep 2017

I. INTRODUCTION

The physics of $S = \frac{1}{2}$ quantum magnets (QM) is extremely rich, owing to the variety of magnetic exchange interaction networks in different systems, as determined by the lattice geometry and the orbital hybridization[1,2]. Systems studied so far include quasi 1D-linear chains, planar 2D-systems (ladders, kagome-layers, triangles or square lattices) or more complex 3D-structures such as the hyperkagome or pyrochlore lattices. Recently, the field of $S = \frac{1}{2}$ quantum magnetism has been extended away from 3d ions (such as those containing Cu^{2+} or V^{4+} ions) towards 4d and 5d systems[1]. In these materials, an effective $j_{\rm eff} = \frac{1}{2}$ moment can be realized due to strong spin orbit coupling (SOC) and in certain compounds the presence of frustration is suspected to lead to a quantum spin liquid (QSL) ground state[3]. In general, having the energy of the SOC, the Coulomb interaction (parameterised by U) and the crystal electric field splitting (CEF) of the same order of magnitude leads to highly degenerate magnetic states and complex excitations for many 4d and 4d QMs. These excitations can be gapless or gapped, but their nature is complicated by the presence of disorder and anisotropic interactions, and their understanding is hindered by the scarcity of model materials[1,3]. One approach to describe the highly degenerate states in such frustrated systems utilizes a fermionic band-like picture with chargeless spinon ($S = \frac{1}{2}$) excitations. The fermionic spinon concept was first introduced in cuprates[4] and for organic Cu-based QSLs[5,6]. It was later established in other QMs, such as spin chains[7], 2D-systems[8–10] and 3D-networks including pyrochlore lattices[11,12].

The honeycomb 4d and 5d planar QMs have become attractive systems to study following the discovery of graphene, a honeycomb, 2D Dirac semimetal (SM); its unique properties stem from its linear dispersive modes ($E \sim k$) and its T-linear density of states at the Fermi level $N(E_F)$[13]. These properties lead to a T^2-behavior in the electronic specific heat ($\propto TN(E_{\rm F})$) and a T^3-power law for the spin-lattice relaxation rate $1/T_1$ ($\propto TN^2(E_{\rm F})$)[13,14]. By analogy 2D-honeycomb QSLs, with linear dispersive fermionic spinon bands and low energy gapless magnetic excitations (spinons or Majorana fermions), are expected to exhibit a T^2-behavior in the magnetic specific heat[15–17] and also power-law spin-lattice relaxation: $1/T_1 \sim T^n$[15–20].

The theoretically-solvable Heisenberg-Kitaev model[21–24] predicts that a honeycomb lattice decorated with $j_{\rm eff} = \frac{1}{2}$ pseudospins can have a QSL ground state. Experimental realizations of this include (Li,Na)$_2$IrO$_3$, and α-RuCl$_3$[25–36]. Na_2IrO_3 displays zig-zag magnetic ordering, while α-Li_2IrO_3 exhibits incommensurate spiral ordering. α-$RuCl_3$ exhibits a complex magnetic ordered state while recent NMR results suggest a gapping out of magnetic excitations towards low temperatures once the order is suppressed by magnetic field[27,32]. Surprisingly, the structural 4d-homologue Li_2RhO_3 also shows insulating behavior in spite of reduced spin-orbit interactions[37] and even more interestingly this system exhibits no sign of long range magnetic ordering (LRO), unlike its Ir counterpart[38]. Magnetic exchange between Rh^{4+}-ions are expected to be highly frustrated, which makes this pseudospin $j_{\rm eff} = \frac{1}{2}$ system a promising candidate for a Kitaev quantum spin liquid. Here we provide a comprehensive account of the local magnetic properties of Li_2RhO_3 probed by ^{7}Li ($I = 3/2$) NMR and μSR accompanied by magnetization and heat capacity measurements down to 0.4 K.

II. RESULTS AND DISCUSSION

Polycrystalline samples of Li_2RhO_3 were synthesized by a method described elsewhere (see the supplemental information[39]). Shown in Fig. 1(a) is the temperature dependence of the *d.c.*-magnetic susceptibility $\chi(T)$ measured following zero-field cooled (ZFC) and field-cooled (FC) proto-

cols at 10 mT. The ZFC and the FC $\chi(T)$ curves split at 6 K, which may arise from short range magnetic order (SRO) due to a partial freezing of Rh-moments. However, the splitting in $\chi(T)$ is small, which indicates that probably only a small fraction of moments participate in the glassy state. SRO effects ("spin freezing") admixed onto the quantum spin liquid state have been discussed in quite a large number of materials, such as $Na_4Ir_3O_8$ and $Ni_2Ga_2S_4$[41–50]. The Curie-Weiss (CW) fit (Fig. 1b) in the range $100 \leq T \leq 300$ K yields an effective moment of 2.2 μ_B per Rh-ion. This is well above the spin-only value for the $S = \frac{1}{2}$ low-spin configuration of the $4d^5$-state of Rh^{4+}, which points towards a moderate spin orbit coupling[37,51,52]. The negative sign of the Curie Weiss temperature $\theta_{CW} = -60$ K suggests the prominence of antiferromagnetic (AFM) correlations between Rh^{4+}-moments. The exchange interaction between the nearest neighbor Rh^{4+}-moments can be determined from the high temperature series expansion (HTSE) frequently used for honeycomb lattices with moderate SOC (such as $4d^5$ Ru^{3+} ions in α-$RuCl_3$). The HTSE yields an AFM interaction of $J/k_B \approx 75 \pm 5$ K and is in reasonable agreement with that obtained from the mean field approximation (MFA)[39,53]. The a.c.-susceptibility exhibits a peak at about $T_g \approx 6$ K[39] and the peak positions are weakly frequency dependent, showing the role of dissipative spin dynamics in driving such a short range spin freezing mechanism. The origin of this partial spin freezing might be related to the presence of local disorder in the lattice of Li_2RhO_3[52,54–56] (see discussion in[39]) and the glassy feature smears out at higher fields ($\mu_0 H > 1$ T)(see Fig. 1b). It may be noted that the spin freezing effect on the magnetization and the heat capacity in Li_2RhO_3 is rather minor in comparison with the textbook spin glass materials[57].

The heat capacity coefficient C_m/T obtained in different magnetic fields is shown in Fig. 2(a). The heat capacity exhibits no signature of LRO down to 0.35 K. The magnetic heat capacity (C_m) was obtained by subtracting the lattice contribution using Li_2SnO_3[see Fig. 2(c)] as a reference. As shown in Fig. 2(a), C_m/T displays a broad maximum at about 10 K, which could be associated with the highly frustrated nature of the system as discussed in spin liquids[1,45,58]. The strength of the exchange coupling and dimensionality of the system accounts for the position of the broad maximum in C_m and it varies as $T/|\theta_{CW}|$ in frustrated magnets. In Li_2RhO_3, we found $T/|\theta_{CW}| \approx 0.16$, which is comparable with those values in other 3d and 5d frustrated magnets[41,45,59]. The magnetic entropy $S_m = \int C_m/T\, dT$ up to 45 K was found to be only 35% [≈ 2.04 J/mol K, Fig. 2(b)] of $R \ln 2$ (≈ 5.76 J/mol K), consistent with the presence of short-range spin correlations. Below 10 K, C_m exhibits a T^2-behavior [Fig. 2(a)] indicating the persistence of spin dynamics with low lying gapless excitations, which is in agreement with the finite value of χ at low T in the context of the QSL state. The T^2-dependence of C_m is frequently found in 4d and 5d quantum magnets as a fingerprint of the spin liquid ground state[23,60,61].

The ^{7}Li NMR powder spectra at 70 MHz shown in Fig. 3(a) show a single Li-NMR line which exhibits a clear broadening towards low temperatures without any strong anisotropy. The spectra consist of superimposed intensities from three

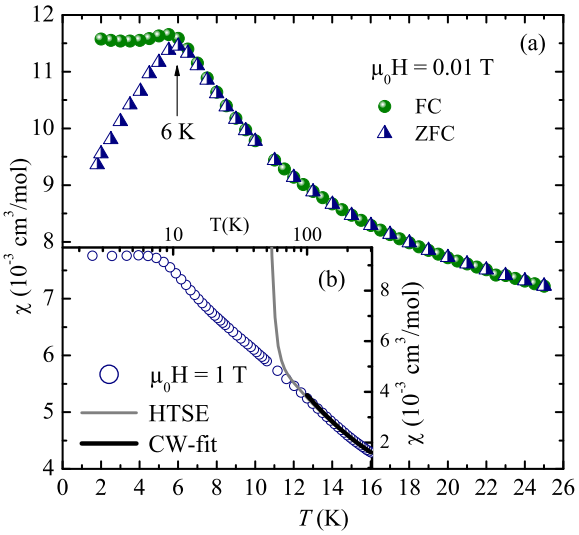

FIG. 1. (Color online) (a) The temperature dependence of the ZFC and FC susceptibility $\chi(T)$ measured in an applied field of 0.01 T. (b) $\chi(T)$ at 1 T, with HTSE (high temperature series expansion) and CW (Curie-Weiss) fits as discussed in the text.

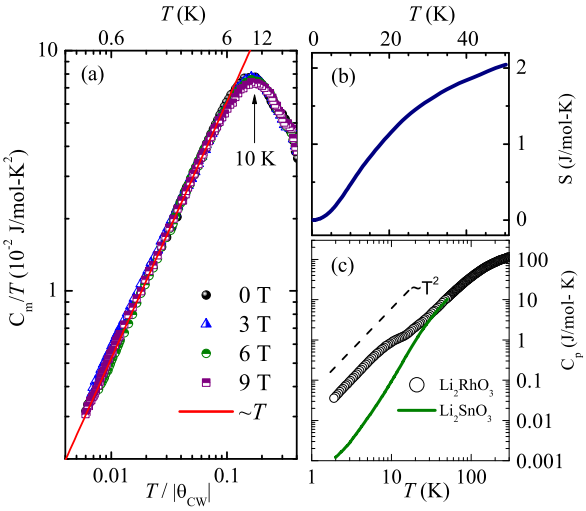

FIG. 2. (Color online) (a) Magnetic heat capacity co-efficient (C_m/T) in various fields as a function of $T/|\theta_{CW}|$. The upper axis shows the absolute T-dependence and the solid line represents a T-linear fit, as discussed in the text. (b) T-dependence of the magnetic entropy in zero field. (c) T-dependence of the total heat capacity in zero field for Li_2RhO_3 compared with the non-magnetic homologue Li_2SnO_3. The dashed line indicates a T^2-behaviour.

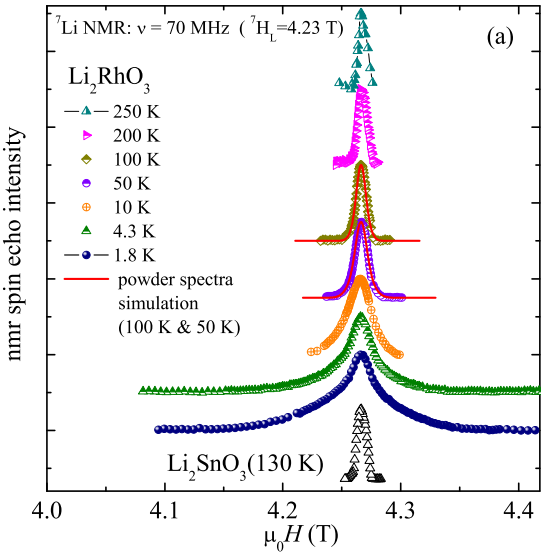

FIG. 3. (Color online) Representative field-swept ^{7}Li-NMR spectra in Li_2RhO_3 at different temperatures (the solid line is a simulation for 100 K and for 50 K). At the bottom of the figure we show the ^{7}Li-NMR spectrum at 130 K for the non-magnetic structural homologue Li_2SnO_3.

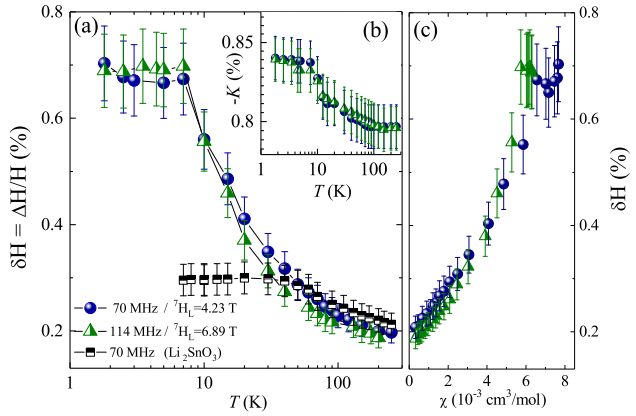

FIG. 4. (Color online) (a) The T-dependence of the full width at half maximum (FWHM) linewidth divided by the resonance field (=relative linewidth, $\delta H = \Delta H/H$) at 70 MHz and 114 MHz compared with $\delta(H)$ of the non-magnetic homologue Li_2SnO_3. (b) T-dependent NMR shift, K, at 70 MHz and 114 MHz. (c) $\delta H(T)$ vs. $\chi(T)$ (obtained at the NMR fields) with T as an implicit parameter. The Larmor fields are calculated by using the ^{7}Li gyromagnetic ratio of 16.5459 MHz/T.

powder averaged Li-lines from the three Li-sites in the lattice structure (see Supplementary Material[39] for more details). The inset of Fig. 4(a) represents the T-dependent NMR shift, $K(T)$, estimated from the simulation of each powder spectrum [see solid line in Fig. 3(a)]. The T-dependence of the shift is reminiscent of the bulk susceptibility [Fig. 1(b)]. $K(T)$ consists of a T-dependent part $K_{\rm Rh}(T)$ due to the coupling of the Rh^{4+} moments with the Li nuclear spins and a nearly a T-independent orbital part $K_{\rm orb}$ which is enhanced due to the presence of moderate spin-orbit interaction[61,62]. The linear scaling between K and χ (given by $K = A_{\rm hf}\chi/N_{\rm A}$) at high-$T$ yields a hyperfine coupling constant $A_{\rm hf} = -(0.3 \pm 0.06)$ kOe/$\mu_{\rm B}$ between the ^{7}Li nucleus and the Rh^{4+} electron spin. Fig. 4(a) shows the NMR linewidth [full width at half maximum (FWHM)] divided by the resonance field (therefore relative linewidth, $\delta H = \Delta H/H$) at two NMR frequencies. The relative linewidth δH exhibits no field dependency and follows the bulk susceptibility [see Fig. 1(b)]. To account for the effect of the first order quadrupolar splitting on the line broadening of the ^{7}Li NMR powder spectra we have investigated the non-magnetic homologue Li_2SnO_3 under the same NMR conditions (see Supplemental Material[39]). This gives clear evidence that the low temperature broadening is a generic feature of Li_2RhO_3 and the scaling with the bulk susceptibility demonstrates the magnetic origin of the broadening. The broadening is associated with static and slow fluctuating hyperfine field contributions at the nuclei sites. It is remarkable that δH is independent of magnetic field. This implies that the absolute width is field dependent, suggesting that at these fields the system is not yet in the fully polarized state and sizeable correlations among Rh^{4+} moments are still present. This is consistent with the absence of LRO in $C_{\rm m}$ down to 0.35 K. The saturation of $\delta H(T)$ at low T indicates the persistence of a quasi-static distribution of local magnetic fields and a slowing down of magnetic fluctuations such that Rh^{4+}-moments fluctuate with a frequency less than the NMR frequency. The fact that above approximately 100 K [see Fig. 4(a) and Supplementary Material[39]] Li_2RhO_3 and Li_2SnO_3 have comparable NMR linewidths, suggests that the effect of anti site order (Li–Rh or Li–Sn) discussed frequently in the literature[63] in the linewidth could be neglected (see discussion in[39]). The magnetic moment of 0.8 μ_B estimated from the NMR linewidth at about 4 K and in a NMR field of 4.23 T (70 MHz) is small compared to the Rh^{4+} Curie-Weiss moment and suggests the presence of strong quantum fluctuations induced by magnetic frustration[43,64]. We found no loss of NMR signal intensity, typical for some disordered materials, which indicates that Li_2RhO_3 is not a conventional spin glass material. This scenario is further supported by the absence of rectangular shaped powder averaged NMR spectra expected for materials that show LRO[65] and moreover by the field independence of the relative linewidth. The quasi-static NMR results presented so far support the scenario of a minority part of moments in a short range like frozen state coexisting with a majority of moments which remain liquid-like and which fluctuate at low-T[41–45].

NMR spin-lattice relaxation rate measurements are very suitable to probe slow spin excitations because in general $1/T_1$ tracks the q-dependent complex dynamic spin susceptibility (see[39] for more details). Fig. 5(a) shows $1/T_1$ vs. T

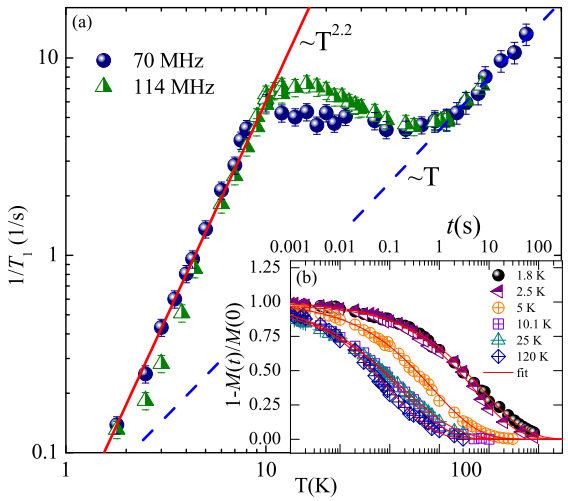

FIG. 5. (Color online) (a) The T-dependence of $1/T_1$ at two NMR frequencies (fields). The solid line indicates a $T^{2.2}$-behavior below 10 K wheras the dashed line depicts the T-linear behavior around 100 K. (b) Longitudinal magnetization recovery curves $M(t)$ at various temperatures in a semi-log plot. The solid curved lines are the individual fits of the data with a stretched exponential function (see Supplemental Materials[39] for more details) at various temperatures.

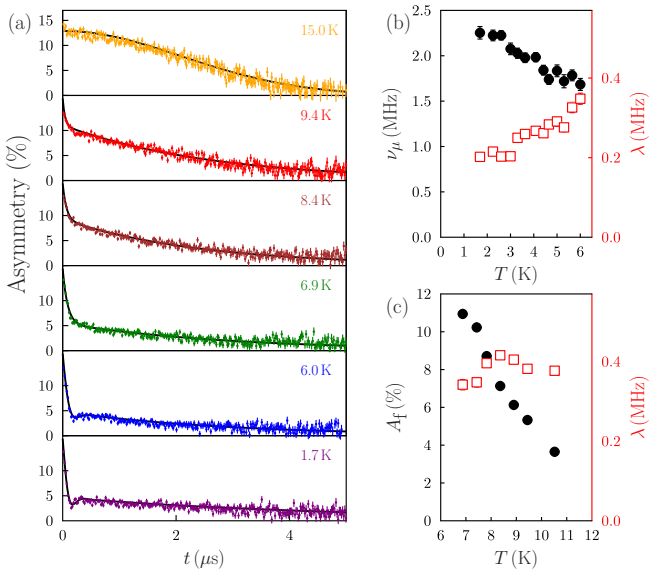

FIG. 6. (Color online) (a) Representative μSR spectra for Li_2RhO_3 measured at a range of temperatures. (b) The fitted precession frequency ν_μ which indicates the average field experienced by the muon in the spin frozen state (solid black circles, left-hand axis) and the relaxation rate λ of the slowly-relaxing component (open red squares, right-hand axis). (c) The amplitude A_f of the fast-relaxing component (solid black circles, left-hand axis) and λ (open red squares, right-hand axis).

at two different NMR frequencies (fields). Towards low temperatures $1/T_1$ decreases linearly with T and passes through a broad maximum around 10 K. This maximum could not be associated with a conventional SG freezing where a critical slowing down of spin fluctuations at T_g leads to a very short T_1 and an NMR signal wipeout at low and intermediate T[43,64]. As shown in Fig. 5(a), $1/T_1$ decreases on further cooling below 10 K and displays a pronounced $T^{2.2}$-behavior down to 1.8 K. In principle, $1/T_1$ tracks the spectral density of the Fourier transform of the time correlation function of the transverse component δh_+ of the fluctuating local field at nuclear sites $h_\pm(0)$ with the nuclear Larmor frequency $\omega_N = \gamma H$ as[66–68] $\frac{1}{T_1} = \frac{\gamma_N^2}{2}\int_{-\infty}^{+\infty}\langle h_\pm(t)h_\pm(0)\rangle e^{i\omega_N t}\,dt$, where γ_N is the gyromagnetic ratio of the nuclear spin. Assuming the time correlation function varies as $e^{-\Gamma t}$, one can express $R = \frac{1}{T_1TK} = A\frac{\Gamma}{\omega_c^2+\omega_N^2}$ where A depends on the hyperfine coupling constant and K is the isotropic NMR shift. Here, ω_c corresponds to the fluctuation frequency of the fluctuating hyperfine field at the ^{7}Li nucleus site transfered from the fluctuating Rh^{4+} moments. One would expect $R \approx 1/\omega_c$ when $\omega_c \gg \omega_N$, while for $\omega_c \ll \omega_N$ one should find that R depends on the NMR field ($R \approx 1/\omega_N$). When $\omega_c = \omega_N$, $R(T)$ approaches a maximum (see Supplemental Materials[39], Fig. S2), which is a consequence of the slowing down of the fluctuation frequency ω_c of Rh^{4+} moments. We find that ω_c is nearly T-independent at high-T, but decreases below 10 K as $\omega_c \propto T^{1.2}$ at low-T, suggesting the slow spin dynamics of Rh^{4+}. This is consistent with the broad NMR line at low-T. The slowing down of spin fluctuations might then dominate the low temperature magnetic properties[42,43]. The power law dependence of $1/T_1$ can be compared with that found in the SOC-driven 5d-spin liquid compound $Na_4Ir_3O_8$[47] and other low dimensional quantum magnets[18,19,64,69,70], which is attributed to the existence of gapless state in the spin excitation spectrum and is in accord with finite value of χ and K, and $C_m \sim T^2$ behavior at low-T. The longitudinal nuclear spin-lattice relaxation rate is given by the low energy (ω) and momentum space (q) integrated hyperfine form factor $A(q,\omega)$ and the imaginary part of the complex dynamic electron susceptibility $\chi''(q,\omega)$ (proportional to $S(q,\omega)$, the dynamic structure factor). For a 2D Kitaev spin liquid calculations of $S(q,\omega)$ suggest either a gapped ($1/T_1 \sim \exp(-\Delta/k_BT)$) or a gapless ($1/T_1 \sim T^n$) behavior[16,18,19]. For Li_2RhO_3, the gapless $T^{2.2}$ power law or alternatively the (pseudo) gapped behavior (i.e., $1/T_1 \sim \exp(-\Delta/k_BT) + \text{constant}$) reasonably fit the $1/T_1$ data (see Supplemental Material[39], Fig. S4).

Our muon-spin rotation (μSR)[71] experiments were carried out at PSI. Representative spectra are shown in Fig. 4(a). For temperatures below about 6 K, there is a single heavily damped oscillatory signal (proportional to $\cos(2\pi\nu_\mu t)e^{-\Lambda t}$) together with a slow relaxation (proportional to $e^{-\lambda t}$). The damped oscillation signifies static magnetic Rh^{4+} moments but the large damping is entirely consistent with moment freezing, and is not associated with long range magnetic ordering. Fluctuations persist at low temperature evidenced by the presence of the slow relaxation. The frequency of the damped oscillation, ν_μ, is around 2 MHz and falls slightly

on warming [see Fig. 4(b)] while the relaxation rate λ rises. At T above $\approx$6 K, it is no longer possible to fit the fast relaxation with a damped oscillation, and we identify this T with the freezing temperature T_g, in agreement with magnetization measurements[37,51] and coinciding with the peak measured in *ac* susceptibility (see Supplemental Material[39]). For $T > T_g$ we fit our data instead using a sum of two exponential relaxations, so that the fitting function becomes $A(t) = A(0)[A_f e^{-\Lambda t} + (1-A_f)e^{-\lambda t}]$. The amplitude of the fast relaxing term A_f falls on warming above 6 K [see Fig. 4(c)] and is entirely absent by 15 K by which temperature the relaxation is dominated by a Gaussian response characteristic of static nuclear moments. These observations indicate that although the freezing disappears above T_g there remain some frozen regions of the sample which persist well above T_g, up to almost $2T_g$, perhaps in small, slowly-fluctuating clusters. These slow fluctuations may likely contribute to the slow relaxation that is observed in these data. The volume fraction of the clusters decreases on warming and this can be directly related to the decrease in A_f. In fact, the observation of a slowly relaxing fraction throughout the temperature range demonstrates that the frozen state possesses some weak dynamics. These measurements are consistent with the development of a moment-frozen state below 6 K at small magnetic fields.

III. CONCLUSION

We have presented a study on the magnetism of Li_2RhO_3 to probe a possible spin liquid ground state and investigate the presence of partial frozen moments. Whereas frozen moments were evidenced by low field susceptibility measurements, the NMR measurements performed in higher field could hardly resolve this effect. The zero field μSR evidences frozen moments but also persistent low energy spin dynamics. χ, δH and K remain finite towards low T wheras the magnetic specific heat as well as the spin lattice relaxation rate exhibit characteristic temperature dependencies assigned to quantum spin liquids. The magnetic heat capacity C_m displays no signature of LRO down to 0.35 K despite an AFM interaction $J/k_B \approx 75$ K between Rh^{4+} moments. The $C_m \sim T^{2.2}$ and the $1/T_1 \sim T^{2.2}$ behavior at low-T might be assigned to gapless excitations as predicted for the Kitaev quantum spin liquid state. Further studies on single crystals are highly recommended to establish whether the partial moment freezing is generic to the system (e.g. because of the proximity of the Kitaev QSL to the magnetic ordered phase) or a matter of sample quality (presence of structural disorder). Nonetheless the study presented here clearly show that Li_2RhO_3 is not a conventional bulk spin glass material, the SRO effects are wiped out in magnetic fields and most important the low-T spin dynamics as well as the specific heat are reminiscent of that of a quantum spin liquid.

IV. ACKNOWLEDGEMENT

We would like to thank A. V. Mahajan, H. Yasuoka, P. Mendels and M. Majumder for fruitful discussions. PK acknowledges support from the European Commission through Marie Curie International Incoming Fellowship (PIIF-GA-2013-627322). SM acknowledges financial support by the Helmholtz Virtual Institute 521 ("New states of matter and their excitations"). FRF, TL and SJB acknowledge support from EPSRC (UK) (Grants EP/M020517/1 and EP/N023803/1). Part of this work was carried out at the Swiss Muon Source (SμS), Paul Scherrer Institut, Villigen, Switzerland.

* Present address: Department of Physics, Indian Institute of Technology, Madras Chennai-600036, India
† Present address: Department of Physics and Astronomy, Iowa State University, Ames, Iowa, USA
‡ corresponding author: baenitz@cpfs.mpg.de

[1] L. Balents, Nature **464**, 199 (2010) and references therein.
[2] S. Sachdev, Nature Physics **4**, 173 (2008).
[3] C. Lacroix, P. Mendels, and F. Mila, *Introduction to Frustrated Magnetism*, Springer Series in Solid-State Sciences (Springer, New York), Vol. **164**. 2011.
[4] J. T. Kheli and W. A. Goddard III, Proc. Natl. Acad. Sci. **90**, 9959 (1993).
[5] S.-S. Lee, P. A. Lee and T. Senthil, Phys. Rev. Lett. **98**, 067006 (2007).
[6] T. Itou, A. Oyamada, S. Maegawa and R. Kato, Nature Physics **6**, 673 (2010).
[7] M. Mourigal, M. Enderle, A. Klöpperpieper, J.-S. Caux, A. Stunault and H. M. Rønnow, Nature Physics **9**, 435 (2013).
[8] J. Nasu, J. Knolle, D. L. Kovrizhin, Y. Motome and R. Moessner, Nature Physics **12**, 912 (2016).
[9] T.-H. Han,J. S. Helton, S. Chu, D. G. Nocera, J. A. Rodriguez-Rivera, C. Broholm and Y. S. Lee, Nature **492**, 406 (2012).
[10] Yao Shen, Y.-D. Li, H. Wo, Y. Li, S. Shen, B. Pan, Q. Wang, H. C. Walker, P. Steffens, M. Boehm, Y. Hao, D. L. Quintero-Castro, L. W. Harriger, M. D. Frontzek, L. Hao, S. Meng, Q. Zhang, G. Chen and J. Zhao, Nature **540**, 559 (2016)
[11] M. J. P. Gingras, and J. E. Greedan, Rev. Mod. Phys. **82**, 53 (2010).
[12] B. Normand and Z. Nussinov, Phys. Rev. B **93**, 115122 (2016).
[13] A. H. Castro Neto, F. Guinea, N. M. R. Peres, K. S. Novoselov, and A. K. Geim, Rev. Mod. Phys. **81**, 109 (2009).
[14] B. Dora, F. Simon, Phys. Rev. Lett. **102**, 197602 (2009) .
[15] Z. Y. Meng, T. C. Lang, S. Wessel, F. F. Assaad and A. Muramatsu, Nature **464**, 847 (2010).
[16] J. Knolle, D.L. Kovrizhin, J.T. Chalker, and R. Moessner, Phys. Rev. Lett. **112**, 207203 (2014).
[17] J. Knolle, D. L. Kovrizhin, J. T. Chalker, and R. Moessner Phys. Rev. B **92**, 115127 (2015).
[18] J. Yoshitake, J.Nasu, and Y. Motome, Phys. Rev. Lett. **117**, 157203 (2016).
[19] X.-Y. Song, Y.-Z. You and L. Balents, Phys. Rev. Lett. **117**, 037209 (2016).
[20] J. Knolle, Dynamics of a Quantum Spin Liquid, Springer Theses, Springer International Publishing, ISBN 978-3-319-23951-4, (2016)

[21] J. Chaloupka, G. Jackeli, and G. Khaliullin, Phys. Rev. Lett. **105**, 027204 (2010).
[22] A. Y. Kitaev, Ann. Phys. (N.Y.) **321**, 2 (2006).
[23] S. Trebst, arXiv: 1701.07056 (2017).
[24] D. Gotfryd, J. Rusnačko, K. Wohlfeld, G. Jackeli, J. Chaloupka, and A. M. Oles, Phys. Rev. B **95**, 024426 (2017)
[25] S. C. Williams, R. D. Johnson, F. Freund, Sungkyun Choi, A. Jesche, I. Kimchi, S. Manni, A. Bombardi, P. Manuel, P. Gegenwart, and R. Coldea, Phys. Rev. B **93**, 195158 (2016)
[26] A. Banerjee, C. A. Bridges, J.-Q. Yan, A. A. Aczel, L. Li, M. B. Stone, G. E. Granroth, M. D. Lumsden, Y. Yiu, J. Knolle, S. Bhattacharjee, D. L. Kovrizhin, R. Moess- ner, D. A. Tennant, D. G. Mandrus, and S. E. Nagler, Nature Materials **15**, 733 (2016).
[27] S.-H. Baek, S.-H. Do, K.-Y. Choi, Y. S. Kwon, A.U.B. Wolter, S. Nishimoto, J. van den Brink, B. Büchner, Phys. Rev. Lett. **119**, 037201 (2017).
[28] S. H Chun, J.-W. Kim, J. Kim, H. Zheng, C. C. Stoumpos, C. D. Malliakas, J. F. Mitchell, K. Mehlawat, Y. Singh, Y. Choi, T. Gog, A. Al-Zein, M. M. Sala, M. Krisch, J. Chaloupka, G. Jackeli, G. Khaliullin and B. J. Kim, Nat. Phys. **11**, 462 (2015).
[29] M. Hermanns, S. Trebst, and A. Rosch, Phys. Rev. Lett. **115**, 177205 (2015).
[30] S. K. Choi, R. Coldea, A. N. Kolmogorov, T. Lancaster, I. I. Mazin, S. J. Blundell, P. G. Radaelli, Y. Singh, P. Gegenwart, K. R. Choi, S.-W. Cheong, P. J. Baker, C. Stock, and J. Taylor, Phys. Rev. Lett. **108**, 127204, (2012).
[31] J. Reuther, R. Thomale, and S. Rachel, Phys. Rev. B **90**, 100405(R) (2014).
[32] M. Majumder, M. Schmidt, H. Rosner, A. A. Tsirlin, H. Yasuoka, and M. Baenitz, Phys. Rev. B **91**, 180401(R) (2015).
[33] T. Takayama, A. Kato, R. Dinnebier, J. Nuss, H. Kono, L.S.I. Veiga, G. Fabbris, D. Haskel, and H. Takagi, Phys. Rev. Lett. **114,** 077202 (2015).
[34] S. Manni, Y. Tokiwa, and P. Gegenwart, Phys. Rev. B **89**, 241102(R) (2014).
[35] S. Manni, Sungkyun Choi, I. I. Mazin, R. Coldea, M. Altmeyer, H. O. Jeschke, R. Valent, and P. Gegenwart, Phys. Rev. B **89**, 245113 (2014).
[36] M. Hermanns and S. Trebst, Phys. Rev. B **89**, 235102 (2014).
[37] I. I. Mazin, S. Manni, K. Foyevtsova, Harald O. Jeschke, P. Gegenwart, and Roser Valent, Phys. Rev. B **88**, 035115 (2013).
[38] Y. Luo, C. Cao, B. Si, Y. Li, J. Bao, H. Guo, X. Yang, C. Shen, C. Feng, J. Dai, G. Cao, and Z. Xu, Phys. Rev. B **87**, 161121(R) (2013).
[39] See Supplemental Material for a.c. susceptibility results and further details of the analysis of spin lattice relaxation rates, which includes Refs. [40].
[40] F. L. Pratt, Physica B **289-290**, 710 (2000).
[41] S. Nakatsuji, Y. Nambu, H. Tonomura, O. Sakai, S. Jonas, C. Broholm, H. Tsunetsugu, Y. Qiu and Y. Maeno, Science **309**, 1697 (2005).
[42] R. H. Colman, F. Bert, D. Boldrin, A. D. Hillier, P. Manuel, P. Mendels, and A. S. Wills, Phys. Rev. B **83**, 180416(R) (2011).
[43] J. A. Quilliam, F. Bert, R. H. Colman, D. Boldrin, A. S. Wills, and P. Mendels, Phys. Rev. B **84** , 180401(R) (2011).
[44] S. Nakatsuji, K. Kuga, K. Kimura, R. Satake, N. Katayama, E. Nishibori, H. Sawa, R. Ishii, M. Hagiwara, F. Bridges, T. U. Ito, W. Higemoto, Y. Karaki, M. Halim, A. A. Nugroho, J. A. Rodriguez-Rivera, M. A. Green and C. Broholm, Science **336**, 559 (2012).
[45] Y. Okamoto, M. Nohara, H. Aruga-Katori, and H. Takagi, Phys. Rev. Lett. **99**, 137207 (2007).
[46] R. Dally, T. Hogan, A. Amato, H. Luetkens, C. Baines, J. Rodriguez-Rivera, M. J. Graf, and S. D. Wilson, Phys. Rev. Lett. **113**, 247601 (2014).
[47] A. C. Shockley, F. Bert, J-C. Orain, Y. Okamoto, and P. Mendels, Phys. Rev. Lett. **115**, 047201 (2015).
[48] Y. J. Uemura, A. Keren, K. Kojima, L. P. Le, G. M. Luke, W. D. Wu, Y. Ajiro, T. Asano, Y. Kuriyama, M. Mekata, H. Kikuchi, and K. Kakurai, Phys. Rev. Lett. **73**, 3306 (1994).
[49] H. D. Zhou, E. S. Choi, G. Li, L. Balicas, C. R. Wiebe, Y. Qiu, J. R. D. Copley, and J. S. Gardner, Phys. Rev. Lett. **106**, 147204 (2011).
[50] T. K. Dey, A. V. Mahajan, P. Khuntia, M. Baenitz, B. Koteswararao, and F. C. Chou, Phys. Rev. B **86**, 140405(R) (2012).
[51] Y. Luo, C. Cao, B. Si, Y. Li, J. Bao, H. Guo, X. Yang, C. Shen, C. Feng, J. Dai, G. Cao, and Z. Xu, Phys. Rev. B **87**, 161121(R) (2013).
[52] V. Todorova and M. Jansen, Z. Anorg. Allg. Chem. **637**, 37 (2011).
[53] H.E. Stanley, Phys. Rev.**158**, 546 (1967); G. S. Rushbrooke and P. J. Wood, Proc. Phys. Soc. A **68**, 1161 (1955).
[54] Y. Singh and P. Gegenwart, Phys. Rev. B **82**, 064412 (2010).
[55] Y. Singh, S. Manni, J. Reuther, T. Berlijn, R. Thomale, W. Ku, S. Trebst, and P. Gegenwart, Phys. Rev. Lett. **108**, 127203 (2012).
[56] S. Manni, PhD thesis: *Synthesis and investigation of frustrated Honeycomb lattice iridates and rhodates*, Georg-August-Universitaet Goettingen (2014).
[57] J. A. Mydosh, *Spin Glasses: An Experimental Introduction* (Taylor and Francis, London,1993).
[58] J. G. Cheng, G. Li, L. Balicas, J. S. Zhou, J. B. Goodenough, Cenke Xu, and H. D. Zhou, Phys. Rev. Lett. **107**, 197204 (2011).
[59] A. P. Ramirez, B. Hessen, and M. Winklemann, Phys.Rev. Lett. **84**, 2957 (2000).
[60] M. J. Lawler, A. Paramekanti, Y. B. Kim, and L. Balents, Phys. Rev. Lett. **101**, 197202 (2008).
[61] Y. Zhou, P. A. Lee, T.-K. Ng, and F.-C. Zhang, Phys. Rev. Lett. **101**, 197201 (2008).
[62] T. K. Dey, A. V. Mahajan, R. Kumar, B. Koteswararao, F. C. Chou, A. A. Omrani, and H. M. Ronnow, Phys. Rev. B **88**, 134425 (2013).
[63] V. M. Katukuri, S. Nishimoto, I. Rousochatzakis, H. Stoll, J. van den Brink, and L. Hozoi, Sci. Rep. **5**, 14718 (2015).
[64] Y. Shimizu, K. Miyagawa, K. Kanoda, M. Maesato, and G. Saito, Phys. Rev. Lett. **91**, 107001 (2003).
[65] Y. Yamada and A. Sakata, J. Phys. Soc. Jpn. **55**, 1751(1986).
[66] T. Moriya, *Spin Fluctuations in Itinerant Electron Magnetism* (Springer, Berlin, 1985).
[67] N. Bloembergen, E. M. Purcell, and R. V. Pound, Nature **160**, 475 (1947).
[68] A. Abragam, *Principles of Nuclear Magnetism* (Oxford University Press, New York, 1983).
[69] T. Imai, E. A. Nytko, B. M. Bartlett, M. P. Shores, and D. G. Nocera, Phys. Rev. Lett. **100**, 077203 (2008).
[70] P. Mendels and F. Bert, J. Phys. Soc. Jpn. **79**, 011001 (2010).
[71] S. J. Blundell, Contemp. Phys. **40**, 175, (1999); S. J. Blundell, Chem. Rev. **104**, 5717 (2004); A. Yaouanc and P. Dalmas de Réotier, *Muon Spin Rotation, Relaxation, and Resonance* (Oxford University Press, Oxford, 2010).

arXiv:1512.04904v4 [cond-mat.str-el] 26 Sep 2017

Supplemental Material: Local Magnetism and Spin Dynamics in the Honeycomb Rhodate Li_2RhO_3

P. Khuntia,[1,*] S. Manni,[2,†] F. R. Foronda,[3] T. Lancaster,[4] S. J. Blundell,[3] P. Gegenwart,[2] and M. Baenitz[1,‡]

[1]*Max Planck Institute for Chemical Physics of Solids, 01187 Dresden, Germany*
[2]*EP VI, Center for Electronic Correlations and Magnetism, Augsburg University, D-86159 Augsburg, Germany*
[3]*Oxford University Department of Physics, Clarendon Laboratory, Parks Road, Oxford OX1 3PU, United Kingdom*
[4]*Durham University, Centre for Materials Physics, South Road, Durham, DH1 3LE, United Kingdom*

(Dated: April 9, 2018)

I. SAMPLE SYNTHESIS, MAGNETIC EXCHANGE AND EFFECT OF LATTICE SITE DISORDER

We have synthesized Li_2RhO_3 polycrystals by the solid state reaction method from stoichiometric amounts of Li_2CO_3 and Rh-powder. The mixture has been pelletized several times and reacted in a flow of O_2 at temperatures up to 850°C. Powder x-ray-diffraction (XRD) scans do not reveal any evidence for secondary phases and are similar to those reported in Refs. 1 and 2. There is no evidence for site mixing between Li and Rh atoms. However, as found for Na_2IrO_3[3], frequent in-plane translational stacking faults along the c-axis are probably present in our sample of Li_2RhO_3. Nevertheless, this is not likely to affect the in-plane 2D physics. Edge-sharing RhO_6 octahedra form a Rh-honeycomb arrangement in which each Rh ion carries a spin-orbit entangled $j_{\rm eff} = \frac{1}{2}$ moment. The lattice structure hosts three different Li-sites (one within and two out of the honeycomb planes[2]).

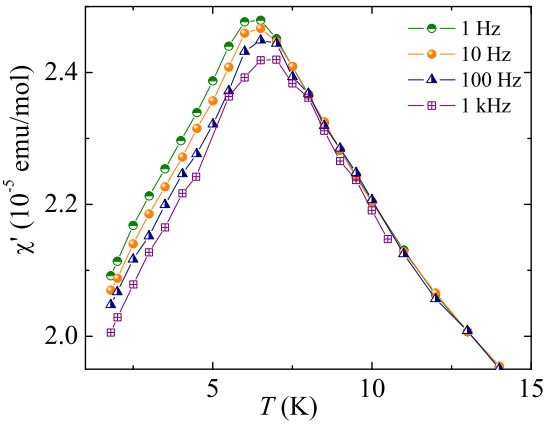

FIG. S1. (Color online) The temperature dependence of the real part of the a.c. magnetic susceptibility at various frequencies.

II. DC- AND AC- SUSCEPTIBILITY

The d.c. magnetic susceptibility (χ=M/H) was measured using a SQUID magnetometer (MPMS, Quantum Design, QD) in the temperature range $1.8 \leq T \leq 300$ K in small magnetic fields ($\mu_0 H \leq 1$ T) where partial spin freezing was found and at 4.23 T and 6.89 T at which NMR measurments were carried out. The frequency and temperature dependence of the a.c. susceptibility data were obtained using a commercial a.c. susceptometer (PPMS, Quantum Design). We found a pronounced peak at T_g= 6 K in the a.c. suceptibility indicative of partial spin freezing, accompanied by a weak frquency dependence reminiscent of a spin glass (see Fig. S1). The effective exchange coupling between Rh^{4+} using mean field theory (MFT) can be estimated as: $J/k_{\rm B} = -3\theta_{CW}/zS(S+1) = 80$ K (with coordination number $z = 3$). This is a very simple and crude estimate given the presence of various exchange couplings in Li_2RhO_3 of comparable strengths[3,4].

For many $S = \frac{1}{2}$ quantum magnets the exchange interaction between the nearest neighbor spins can be described by a Heisenberg type hamiltonian, $H = J\sum_{<i,j>} S_i \cdot S_j$. The magnetic susceptibility at high temperatures can be modelled by the high temperature series expansion (HTSE). For pseudospin $s = \frac{1}{2}$ Rh^{4+} ions with moderate SOC on the honeycomb lattice the model is of some use (especially if the exchange is predominant antiferromagnetic and the Kitaev term is small) and the susceptibility is then given by

$$\chi = \frac{N_A g^2 \mu_B^2}{4k_B T} \sum \left(\frac{J}{k_B T}\right)^n, \qquad (1)$$

where $n = 0.5$ and a_n are series coefficients, the values of which can be found in Ref. 6. We obtain $J/k_{\rm B} \approx (75 \pm 5)$ K, which is close to that estimated using MFT. Given the simplicity of the model and appreciable spin orbit interactions with $J_{\rm eff} = \frac{1}{2}$, the obtained coupling constant is a rough estimate. It may be noted that the HTSE is strictly valid only for $S = \frac{1}{2}$ systems in the absence of spin orbit interactions.

III. ^{7}LI NMR: LINEWIDTH ANALYSIS AND SPIN-LATTICE RELAXATION

NMR is a useful local probe for spin dynamics and local disorder. The local disorder (due to defects, vacancies or anti site order) usually shows in an enhanced NMR linewidth δH, whereas the dynamical information arises via the spin lattice relaxation rate which reflects the fluctuation of hyperfine fields. The NMR spectra and spin-lattice relaxation measurements at two frequencies were carried out using a standard pulsed NMR spectrometer.

The T-dependence of δH in Li_2RhO_3 was compared with that measured in the non-magnetic reference Li_2SnO_3. This

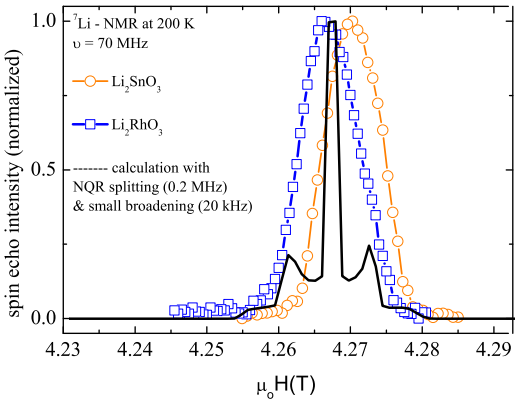

FIG. S2. (Color online) ^{7}Li -powder spectra at 200 K for Li_2RhO_3 and the non magnetic homologue compound Li_2SnO_3. In addition a single Li-site calculation of the spectra with negligibly small broadening is shown by the solid line.

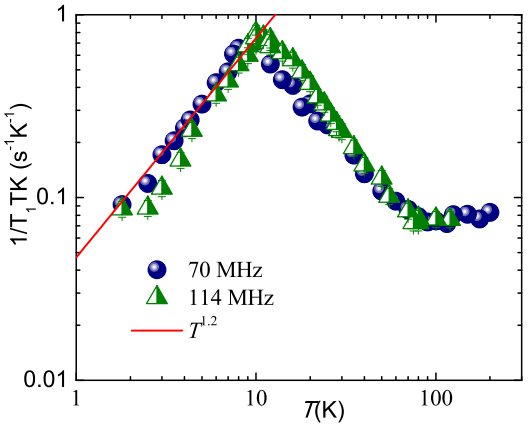

FIG. S3. (Color online) The temperature dependence of $1/(T_1TK)$ at two NMR frequencies.

allows the investigation of the effect of the quadrupolar broadening on the spectra. The linewidth of Li_2RhO_3 ($\delta H = \delta H_{4d} + \delta H_Q$) has a T-dependent contribution (δH_{4d}) related to the underlying Rh magnetism, plus a (nearly) T-independent contribution (δH_Q) arising from the (powder averaged) quadrupolar transitions of the $I = \frac{3}{2}$ quadrupolar ^{7}Li nuclei. For Li_2SnO_3 the linewidth originates only from the quadrupole effect ($\delta H_{4d} = 0$). As seen in Fig. 3, the magnetic brodening in Li_2RhO_3 becomes dominant below approximately 50 K (where δH_Q saturates) wheras towards higher temperatures the linewidth mainly originates from the T-dependence of the quadrupole contribution.

To illustrate this we have shown the ^{7}Li-NMR lines at 200 K for both compound together in Fig. S2. In addition a model calculation for the quadrupolar-split NMR line is shown. Both lines are of equal width, but one should note

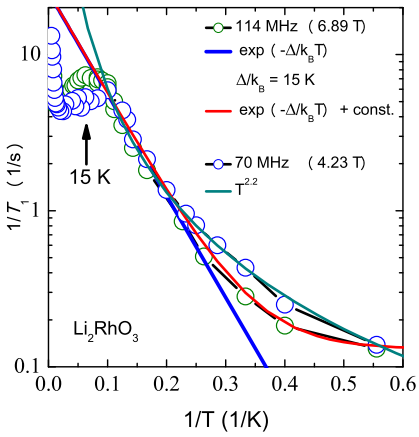

FIG. S4. (Color online) Arrhenius plot for the NMR relaxation rate for the two NMR frequencies together with different fitting functions (see text).

that there are three different Li positions in the structure (one within and two out of the honeycomb planes[2]) which also (beside the powder average) lead to some averaging of the total spectra. Having this in mind it is quite surprising that both lines are relatively narrow and exhibit nearly no spectral anisotropy. The equal linewidth at high temperatures also gives evidence for the absence of anti-site order (Li-Rh and Li-Sn site mixing) frequently discussed in the literature.

The spin lattice relaxation measurements were performed following the saturation recovery method using short *rf* pulses. In Li_2RhO_3, the recovery of longitudinal nuclear magnetization, $M(t)$, at time t after the saturation pulse could be fitted with $1 - M(t)/M(\infty) = e^{-(t/T_1)^\beta}$ (here $M(\infty)$ is the saturation magnetization, and β (≈ 0.5) is the stretch exponent, which is found to be independent of temperature here). This function arises when there is a distribution of relaxation times. The spin-lattice relaxation rate, $1/T_1$ at each temperature is determined by fitting the nuclear magnetization $M(t)$ using the stretched exponential function (see Fig. 5(b)). A non-exponential autocorrelation function is frequently found in quantum spin liquids, but is also common in disordered materials. In general, $1/T_1$ probes the q-averaged low energy spin excitations and $1/(T_1T)$ can be expressed as the wave-vector q-summation of the imaginary part of the dynamic electron spin susceptibility $\chi''(q,\omega_n)$: $\frac{1}{T_1T} \propto \sum_q \mid A_{hf}(q) \mid^2 \frac{\chi''(q,\omega_n)}{\omega_n}$. Here, $A_{hf}(q)$ is the form factor of the hyperfine interactions and ω_n is the nuclear Larmor frequency[7]. Fig. S3 shows the temperature dependence of $R(T) = 1/(T_1TK)$ as a sort of "on site" fluctuation rate. Above 100 K, $R(T)$ is constant which indicates local moment magnetism, consistent with the Curie-Weiss behaviour of the susceptibility. However, towards low temperatures strong correlations between Rh moments set in which is reflected by an increase of $R(T)$. Around 10 K these correlations start dying out towards low temperatures which indicates a slowing down of spin fluctuations. One way to

discuss whether the ground state is spin gapped or gappless is the Arrhenius type of plot (see Fig. S4). Here the experimental data points from Fig. 5 in the main text are replotted together with the $T^{2.2}$ power law and the simple equation for excitations across a gap without ($1/T_1 \sim \exp(-\Delta/k_BT)$, shown by the straight line in Fig. S4) and with a residual (constant) value. A residual $1/T_1$ value might originate from a weak additional Heisenberg type of exchange coupling. Furthermore, a sizable gap anisotropy might also lead to a residual value of T_1. Within the experimental accuracy, we cannot distinguish between a $T^{2.2}$ power law and a pseudogapped behaviour (including a residual value of the relaxation rate) in the spin-lattice relaxation rate. Therefore, our conclusion is that our NMR measurements are probing gapless excitations, consistent with the specific heat results.

IV. MUON-SPIN ROTATION

The muon-spin rotation (μSR) measurments on the polycrystalline sample of Li_2RhO_3 shown in Fig. 6 of the main paper were carried out on the general-purpose spectrometer (GPS) at the Swiss Muon Source (SμS) at PSI (Switzerland). The μSR data were analyzed using the analysis software WiMDA[8]. In a μSR experiment spin-polarized muons are implanted into a sample, where they Larmor precess around the local magnetic field at the muon stopping site. By measuring the angular distribution of the decay product positrons the spin polarization can be tracked. In the case of long-range magnetic order, coherent magnetic fields at particular muon stopping sites within the unit cell lead to oscillatory signals with frequencies dependent on the local magnetic fields at each site. In μSR, impurity phases only contribute according to their volume fraction, and so the technique is an effective measure of intrinsic behavior.

* Present address: Department of Physics, Indian Institute of Technology, Madras Chennai-600036, India
† Present address: Department of Physics and Astronomy, Iowa State University, Ames, Iowa, USA
‡ corresponding author: baenitz@cpfs.mpg.de

[1] V. Todorova and M. Jansen, Z. Anorg. Allg. Chem. **637**, 37 (2011)
[2] S. Manni, PhD Thesis: *Synthesis and investigation of frustrated Honeycomb lattice iridates and rhodates* (2014), available at http://hdl.handle.net/11858/00-1735-0000-0022-5F49-5
[3] S. K. Choi, R. Coldea, A. N. Kolmogorov, T. Lancaster, I. I. Mazin, S. J. Blundell, P. G. Radaelli, Y. Singh, P. Gegenwart, K. R. Choi, S.-W. Cheong, P. J. Baker, C. Stock, and J. Taylor, Phys. Rev. Lett. **108**, 127204, (2012).
[4] I. I. Mazin, S. Manni, K. Foyevtsova, Harald O. Jeschke, P. Gegenwart, and Roser Valent, Phys. Rev. B **88**, 035115 (2013).
[5] J. A. Mydosh, *Spin Glasses: An Experimental Introduction* (Taylor & Francis, London,1993).
[6] H.E. Stanley, Phys. Rev.**158**, 546 (1967); G. S. Rushbrooke and P. J. Wood, Proc. Phys. Soc. A **68**, 1161 (1955).
[7] T. Moriya, *Spin Fluctuations in Itinerant Electron Magnetism* (Springer, Berlin, 1985).
[8] F. L. Pratt, Physica B **289-290**, 710 (2000).